Phase Equilibria of Polypropylene Samples with Hydrocarbon Solvents at High Pressures

C. DARIVA,[1] J.VLADIMIR OLIVEIRA,[1] F. W. TAVARES,[2] J. C. PINTO[1]

[1] Programa de Engenharia Química/COPPE, Universidade Federal do Rio de Janeiro, Cidade Universitária, CP:68502, Rio de Janeiro, 21945-970 RJ, Brazil

[2] Departamento de Engenharia Química, Escola de Química, Universidade Federal do Rio de Janeiro, Cidade Universitária, Rio de Janeiro, 21949-900 RJ, Brazil

Received 28 August 2000; accepted 28 November 2000

ABSTRACT: The objective of this work is to provide high-pressure phase equilibrium data for polypropylene (PP) samples (two commercial and one metallocenic grades) with some hydrocarbon solvents (propane, propylene, *n*-butane and 1-butene). The experiments were carried out in a high-pressure variable-volume view cell in the temperature range of 75–150°C, for polymer compositions ranging from 0.3 to 10 wt %. Phase transitions were recorded visually as cloud points and identified as liquid–liquid and vapor–liquid transitions. When pressure transition data obtained for olefins and paraffins of similar chain length and at similar temperatures and polymer compositions are compared, it may be observed that paraffins lead to the decrease of the pressure transition values. Therefore, the one-phase region is larger for paraffins than for olefins. In the range of commercial interest analyzed, it is also observed that the influence of polymer average molecular weight upon the cloud points is negligible. Experimental data are then used to build the P-T diagrams for these systems, allowing the identification of the LCST (Lower Critical Solution Temperatures) and LCEP (Lower Critical End Points) curves. Finally, the original SAFT equation of state (SAFT-EOS) is used to model the experimental data. It is shown that the SAFT-EOS provides an excellent description of the solution behavior in the whole experimental range analyzed. J Appl Polym Sci 81: 3044–3055, 2001

Key words: polypropylene; hydrocarbon solvent; high pressure; phase equilibrium; SAFT equation of state

INTRODUCTION

The thermodynamics of polymer systems plays an important role in most polymerization processes, and very often is a key factor for polymer production, processing, and material development. The proper understanding of thermodynamic equilibrium of polymer solutions allows the development of techniques for in-line monitoring and control of polymerization reactions[1] and the interpretation of kinetic data and molecular weight distributions (MWD) obtained in heterogeneous polymerizations.[2,3] Recently, efforts have been made to characterize how the thermodynamic behavior of polymer solutions affects the morphology of the final polymer powder obtained when heterogeneous polymerizations are carried out at low and high pressures.[4–7]

Correspondence to: J. C. Pinto (pinto@peq.coppe.ufrj.br).
Contract grant sponsors: CNPq and FAPERJ.

Journal of Applied Polymer Science, Vol. 81, 3044–3055 (2001)

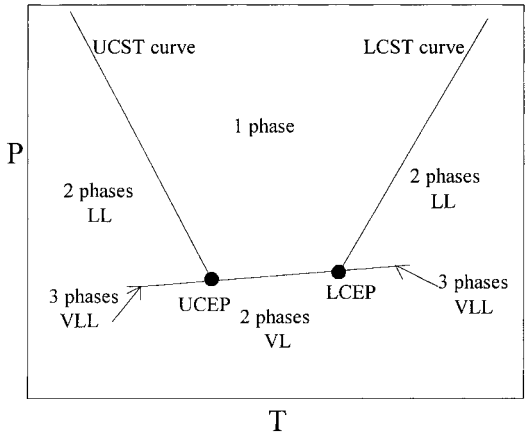

Figure 1 Typical high-pressure phase equilibrium diagram for polymer–solvent systems.

The phase behavior of polymer solutions depends strongly on the energetic interactions and on the size differences between polymer and solvent molecules. At temperatures close to the solvent critical point, polymer precipitates due to the much larger thermal expansion coefficient of the solvent (free volume effect), when compared to that of the polymer. This type of phase split is known as the Lower Critical Solution Temperature (LCST) phase transition. The LCST is characterized by the increase of pressure transition values with temperature $[(\partial P/\partial T)_x > 0]$, as the hydrostatic pressure decreases the free volume differences between the polymer and solvent, and hence, makes them more compatible. At lower temperatures, differences of energetic interactions between polymer and solvent molecules may lead to limited polymer solubility and phase split, known as the Upper Critical Solution Temperature (UCST) phase transition.[8,9] Figure 1 presents a typical P-T diagram for an amorphous polymer–solvent system.

As pointed out by Folie and Radosz,[10] it must be noticed that LCST and UCST curves are not actual critical loci but are labeled LCST and UCST because they correspond to the lower and upper boundaries in T-x coordinates, respectively. In the P-T projection, these boundaries intersect the VL (vapor–liquid) equilibrium curve near the LCEP (Lower Critical End Point) and UCEP (Upper Critical End Point), respectively. In general, the VL curve is close but not identical to the solvent vapor pressure. Two different three-phase (VLL—vapor–liquid–liquid) regions are shown in Figure 1. The first one is located below the UCEP temperature condition, while the second one is above the LCEP temperature condition. For temperatures between the UCST and LCST curves, only one phase is present. Sometimes the UCST may be located at such low temperatures that the solution may intersect the polymer solidification boundary before phase separation occurs.[11]

Due to the enormous economic importance of the polyolefin business (more than 80 million metric tons and more than 50 billions U.S. dollars worldwide per year[12]), the thermodynamic study of polyolefin systems has received a lot of attention in the open literature. The most extensively studied polymer systems over the past 30 years certainly are solutions of polyethylene (PE) in hydrocarbon solvents. Folie and Radosz[10] reviewed the phase equilibria of ethylene homopolymer and copolymer materials in supercritical solutions. Cloud point data for other polyolefin systems have also been reported in the literature.[13–18] However, despite the economic importance of the polypropylene (PP) market and rapidly growing installed production capacity of PP plants, investigations about the high-pressure phase equilibrium of PP solutions have hardly been presented in the literature.

To the best of our knowledge, the only experimental data available for high-pressure phase equilibria of PP solutions are those presented by Whaley et al.[19] and Dariva et al.[20]. Whaley et al.[19] studied the phase equilibria of the PP–propane system for polymer samples of different average molecular weights, measured the LCST for different conditions, and concluded that phase equilibria were sensitive to variations of the average molecular weight and stereoregularity of the polymer samples. However, some of the samples used were atactic, and had low weight-average molecular weight (29,000 g/gmol), which are not of commercial interest. Therefore, from a practical point of view, variation of polymer properties of polymer samples analyzed by Whaley et al.[19] was too large. Dariva et al.[20] studied the phase equilibria of PP–hydrocarbon systems, for solutions of propane, propylene, *n*-butane, 1-butene, and toluene. They measured the LCST and the LCEP for different conditions. When experimental data obtained for paraffins and olefins with similar chain lengths were compared, it was observed that the use of paraffins led to a decrease of cloud-point pressures, causing the increase of the one-phase region. For ternary systems containing toluene as a cosolvent, two-phase regions in the P-T diagram were reduced and cloud-point curves were shifted

towards lower pressures as the toluene content was increased.

As pointed out by Whaley et al.,[19] successful semiquantitative calculations of LCST loci were made over 20 years ago by Patterson and coworkers[21,22] and by Chen and Radosz[15] on the basis of the Paterson/Flory approach.[23] Also, lattice models (like Sanchez and Lacombe[24] and Mattedi et al.[25]) have been employed successfully to model phase equilibrium in systems containing polymers. More recently, Chapman and coworkers[26] and Huang and Radosz[27,28] presented the SAFT equation of state (SAFT-EOS), which has been extensively employed to model the phase equilibria of polymer/solvent systems. Regarding polyolefins solutions specifically, the SAFT-EOS has been used very successfully to describe the behavior of solutions containing polyolefins (mostly polyethylene homopolymers and copolymers) at low and high pressures.[14–18]

Despite the importance of polypropylene homopolymers, however, very little has been made about the thermodynamic modeling of phase behavior of PP solutions, probably due to the lack of experimental data. Whaley et al.[19] used the lattice approach of Sanchez and Lacombe[24] to provide a qualitative description of the experimental LCST obtained. Although simulation results obtained were used to support some of the arguments discussed in that work, the quantitative agreement between experimental and simulation results was poor (perhaps because polymer samples were too different). Dariva et al.[20] did not try to model the experimental results obtained in their work.

In this context, this work has two main objectives. The first objective is to provide new high-pressure phase equilibrium data for commercial PP grades in hydrocarbon solvents (propane, *n*-butane, propylene and 1-butene) often used in the olefin industry, in a wide range of temperatures and pressures and for polymer compositions ranging from 0.3 to 10 wt %. Results obtained by Dariva et al.[20] for a commercial Ziegler-Natta PP grade (grade T) are regarded as a benchmark, for comparison with results obtained for different Ziegler-Natta (grade K) and matallocene (grade M) PP grades. Special attention is given to the identification of the LCST curves and to the influence of toluene upon the thermodynamic behavior of PP solutions. (Toluene is used very often as solvent and/or catalyst carrier for kinetic studies.) The second objective is to provide a framework for quantitative description of phase equilibria of PP/hydrocarbon systems. The original SAFT-EOS is used here to model the experimental data obtained. The choice of the SAFT-EOS sounds very natural if one takes into account the fact that the lattice model studied by Whaley et al.[19] did not allow the quantitative description of the measured experimental data and that the SAFT-EOS has been used quite successfully to describe other polyolefins solutions.

It is shown here that paraffins lead to the decrease of the pressure transition values for all polymer samples analyzed, when pressure transition data obtained for olefins and paraffins of similar chain length and at similar temperatures and polymer compositions are compared. This confirms the results obtained previously by Dariva et al.[20] for grade K. Therefore, the one-phase region is larger for paraffins than for olefins, regardless of the polymer sample analyzed. In the range of commercial interest, it is also observed that the influence of polymer average molecular weight upon the cloud points is negligible. Finally, it is shown that the SAFT-EOS provides excellent fits for available experimental data, and may be used successfully for description of the solution behavior in the whole experimental range analyzed.

EXPERIMENTAL

Materials

The solvents used in this work were propylene (C.P. grade, +99.5% pure), propane (analytical grade, +99.5% pure), 1-butene (C.P. grade, +99.0% pure) and *n*-butane (C.P. grade, +99.5% pure). All solvents were purchased from AGA S.A., Rio de Janeiro. The two commercial polypropylene (PP) samples analyzed here (grades K and T) were produced with supported high-activity Ziegler-Natta catalysts, and were generously supplied by Polibrasil Resinas S.A., Rio de Janeiro. The metallocene PP (grade M) was prepared at the Instituto de Macromoleculas, Universidade Federal do Rio de Janeiro, Rio de Janeiro, using the catalyst Me_2Si(2-ethyl,4-phenyl,1-indenyl)$_2ZrCl_2$.

The weight average molecular weights (M_w) of the PP samples were equal to 245,000 g/gmol (PP-T), 476,000 g/gmol (PP-K) and 200,000 g/gmol (PP-M). The polydispersity (PD = M_w/M_n) of the PP samples were equal to 5.0 (PP-T), 4.7 (PP-K), and 2.6 (PP-M). Molecular weight distributions (MWD) were characterized through Gel Perme-

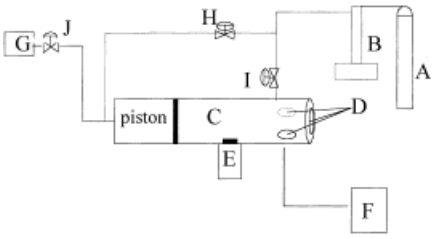

Figure 2 Schematic diagram of the experimental apparatus used for equilibrium measurements. A—Solvent cylinder; B—syringe pump; C—equilibrium cell; D—sapphire windows; E—magnetic stirrer; F—white light source; G—pressure transducer; H—ball valve; I—micrometering valve; J—relief valve.

ation Chromatography (GPC) in a Waters-150CV chromatograph, equipped with 4 Ultra-styragel separation columns (10^3–10^4–10^5–10^6 Å) from Waters. Polymer samples were dissolved in 1,2,4-Benzene Trichloride (TCB), and measurements were performed at 140°C. Polystyrene standards provided by Polymer were used to calibrate the GPC. Dariva[29] presents the GPC spectra of the polymer samples analyzed.

The degrees of isotacticity of the PP samples were equal to 0.96 (PP-T), 0.87 (PP-K), and 0.98 (PP-M). Degrees of isotacticity were measured as the molar fraction of isotactic dyads through ^{13}C-NMR analysis in a Varian Inova-300 equipment, at frequencies of 75.4 MHz. The time interval used for analysis was equal to 10 s. Polymer samples were dissolved in TCB, and measurements were performed at 95°C. NMR spectra of the polymer samples are presented by Dariva.[29]

Differential Scanning Calorimetry (DSC) analysis were performed on Perkin-Elmer DSC 500 equipment, and indicate that the melting temperature (T_m—peak value) is around 159.3, 160.4, and 152.0°C for samples PP-T, PP-K, and PP-M, respectively. DSC spectra obtained are presented by Dariva.[29] DSC spectra were collected after heating PP samples up to 175°C and cooling PP samples down to ambient temperature. Heating and cooling rates were equal to 1°C / min.

Apparatus

The experimental apparatus and procedure used in this study are described in detail elsewhere.[20,30] Phase equilibrium experiments (cloud points) were performed in a high-pressure variable-volume view cell. A schematic diagram of the experimental setup is presented in Figure 2. The apparatus consists basically of a view cell with three sapphire windows for visual observations, an absolute pressure transducer (Smar, LD 301), with a precision of ±0.012 MPa, a portable programmer (Smar, HT 201) for the pressure data acquisition, and a syringe pump (ISCO, 260D). The equilibrium cell has a maximum internal volume of 28 cm^3, and contains a movable piston, which permits the pressure control inside the cell. Phase transitions were recorded visually through manipulation of the pressure behind the piston, using the syringe pump and the solvent (propylene, propane, 1-butene, or *n*-butane, depending on the system under study) as pressurizing fluid. The cell is equipped with an electrical heater and a PID temperature controller (Dextron, DTS4). The controller is connected to a thermocouple, which is in direct contact with the fluid mixture inside the cell body. This arrangement provided a temperature control with a precision of 0.5°C. The experimental apparatus was employed to conduct the experiments up to 270 bar and 150°C.

Procedure

Depending on the desired global composition, an amount of polymer was weighed on a high precision scale balance (Ohaus Analytical Standard, with 0.0001g accuracy) and loaded into the cell. Then, the cell and all lines were flushed with low-pressure gas to remove residual air. Afterwards, the solvent was pumped into the cell to reach the preestablished global composition. The amount of solvent charged was monitored continuously through weighing of the total mass of the transfer vessel of the pump. During the charging process no pressure was applied behind the piston to ensure that the experiments were started with the cell at its maximum volume. Then, the cell content was kept at continuous agitation with the help of a magnetic stirrer and a Teflon-coated stirring bar. After reaching the desired temperature, cell pressure was increased by applying pressure on the back of the piston with the syringe pump until observation of a single phase. At this point, the cell pressure was decreased slowly until incipient formation of a new phase. The equilibrium pressure was then recorded, after repetition of the experimental procedure at least four times, leading to an average reproducibility of 0.70 bar. After completing the test at a given temperature, the cell temperature was stabilized at a new value and the experimental procedure was repeated.

Table I Experimental Results for PP-K

Polymer wt %	T (°C)	P (atm)	Equilibrium Type
	PP-K/1-Butene		
0.983	150	131.0	LL
	140	116.7	LL
	130	98.6	LL
	120	80.5	LL
	110	61.6	LL
	100	41.9	LL
	90	20.3	LL
4.958	150	132.3	LL
	140	116.9	LL
	130	10.9	LL
	120	85.7	LL
	110	63.7	LL
	100	43.2	LL
	90	21.0	LL
7.432	150	132.4	LL
	140	116.0	LL
	130	99.1	LL
	120	82.5	LL
	110	62.8	LL
	100	41.9	LL
	90	21.0	LL
	PP-K/*n*-Butane		
0.995	150	111.9	LL
	140	95.9	LL
	130	80.2	LL
	120	60.0	LL
	110	40.6	LL
	100	22.7	LL
	90	15.4	VL
4.975	150	113.2	LL
	140	98.0	LL
	130	82.3	LL
	120	—	—
	110	42.1	LL
	100	22.7	LL
	90	15.7	VL
7.318	150	111.3	LL
	140	—	—
	130	79.8	LL
	120	61.2	LL
	110	41.2	LL
	100	21.8	LL
	90	15.7	VL

EXPERIMENTAL RESULTS

The new experimental data obtained in this work for grades PP-K and PP-M are given in Tables I to III. Experimental values obtained for PP-T are given elsewhere.[20] For all systems reported in the

Table II Experimental Results for the PP-M/1-Butene System

Polymer wt %	T (°C)	P (atm)	Equilibrium Type
0.285	150	112.5	LL
	140	97.3	LL
	130	82.1	LL
	120	63.8	LL
	110	46.0	LL
	100	27.7	LL
	95	19.6	LL
	90	16.4	VL
	85	14.6	VL
	80	13.2	VL
	75	11.9	VL → S*
0.992	150	127.3	LL
	140	111.3	LL
	130	93.9	LL
	120	75.7	LL
	110	56.4	LL
	100	36.7	LL
	95	26.5	LL
	90	17.75	VL
	85	15.75	VL
	80	13.8	VL
	75	12.1	VL → S
4.932	150	129.2	LL
	135	104.4	LL
	130	95.7	LL
	120	78.1	LL
	110	59.1	LL
	100	37.8	LL
	90	19.8	LL
	85	16.9	VL
	80	15.5	VL
	75	14.4	VL
7.434	150	124.5	LL
	140	108.0	LL
	130	90.6	LL
	120	73.1	LL
	110	54.3	LL
	100	33.9	LL
	95	24.9	LL
	90	18.1	VL
	85	16.6	VL
	80	15.2	VL
	75	14.5	VL → S
9.885	150	122.1	LL
	140	106.6	LL
	130	89.2	LL
	120	72.1	LL
	110	52.8	LL
	100	32.3	LL
	95	23.7	LL
	90	16.6	VL
	85	15.4	VL
	80	13.9	VL
	75	12.6	VL → S

S* → appearance of a solid phase.

Table III Experimental Results for the PP-M/ Propylene System

Polymer wt %	T (°C)	P (atm)	Equilibrium Type
0.294	110	241.2	LL
	105	232.8	LL
	100	223.5	LL
	95	215.2	LL
	90	207.0	LL
	85	198.5	LL
0.975	110	249.7	LL
	105	241.1	LL
	100	233.5	LL
	95	224.2	LL
	90	215.6	LL
	85	207.7	LL
3.012	110	257.5	LL
	105	248.5	LL
	100	240.0	LL
	95	229.8	LL
	90	220.2	LL
	85	212.3	LL
4.888	110	257.9	LL
	105	248.6	LL
	100	240.2	LL
	95	230.9	LL
	90	221	LL
	85	212.8	LL
7.329	110	249.4	LL
	105	241.0	LL
	100	232.6	LL
	95	225.0	LL
	90	216.3	LL
	85	206.7	LL
9.786	110	245.4	LL
	105	237.5	LL
	100	229.2	LL
	95	220.0	LL
	90	211.2	LL
	85	201.9	LL

Solvent effect.

subsequent sections, at least two transition types are present: L to LL and L to VL. By definition, the experimental L to LL phase separation curves obtained here are labeled as LCST. LCST curves finish at the lower temperature region, where either L to VL or L to SL transitions are observed. L to SL transitions were assumed to occur when the turbidity of the polymer suspension did not disappear even after the increase of the cell pressure up to 275 atm. It is assumed here that the crystallization boundary is reached when the increase of the cell pressure up to 275 atm does not allow the restoration of the one-phase region.

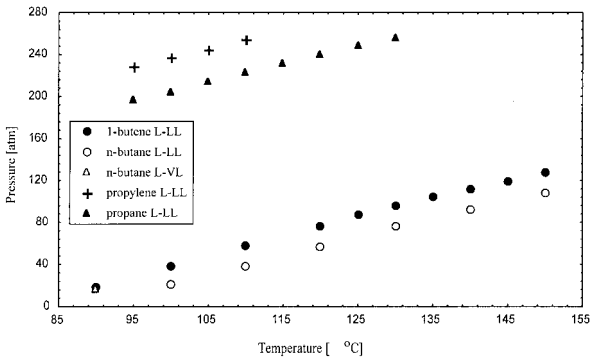

Figure 3 PT diagram of PP-T (5 wt %) with hydrocarbon solvents.

Figure 3 depicts the PT diagram (L to LL phase separation) for PP-T with 1-butene, *n*-butane, propylene, and propane. In this figure polymer concentration is kept constant around 5 wt %. One can observe that the chain length of the solvent affects significantly the phase behavior of the system: when C4 solvents are employed, one-phase regions are much larger than the ones obtained with the C3 solvents. Another evident effect shown in this figure is that olefins increase cloud-point pressures and enlarge the two-phase region, when compared to alkanes with the same chain length. Also, the difference between the cloud point pressure from olefins to paraffins is more pronounced for C3 than for C4 solvents. Figure 4 presents the Px diagram (transition from L to LL) for these systems at constant temperature of 110°C, where the above-mentioned effects are noticed for all compositions analyzed. An interesting effect displayed in Figure 3 is that the solid transition temperatures observed for C4 solvents are slightly lower than the ones observed

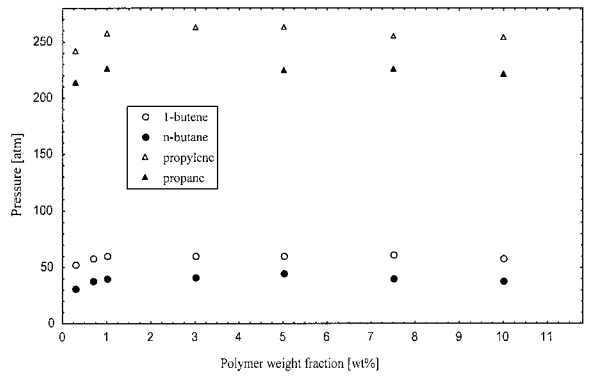

Figure 4 Px diagram (L to LL) of PP-T (110°C) with hydrocarbon solvents.

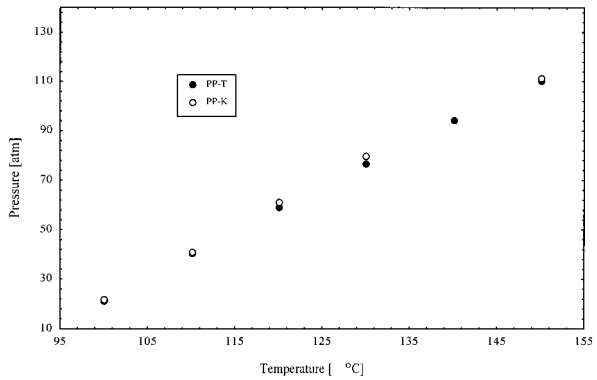

Figure 5 PT diagram (L to LL) with *n*-butane as solvent for PP-T and PP-K (polymer weight fraction kept constant around 7.5 wt %).

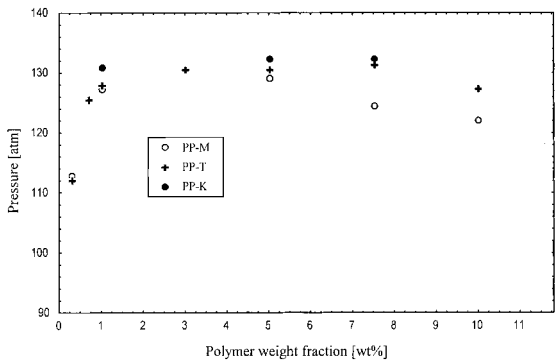

Figure 6 Px diagram (L to LL) for different PPs (150°C) with 1-butene as the solvent.

for C3 solvents, probably due to the higher solvent power exhibited by C4 solvents.

Figure 5 presents the PT diagram (PP concentration around 7.5 wt %) for the two commercial Ziegler-Natta PP grades, using *n*-butane as the solvent. From this figure, one can observe that the polymer molecular weight (from 245,000 g/gmol for PP-T to 475,000 g/gmol for PP-K) has a very small effect upon the LL cloud-point curves. Chen and Radosz[15] investigated the phase behavior of PEP (poly(ethylene-*co*-propylene)) of different weight-average molecular weights (from 790 to 90,000 g/gmol) in olefin solvents, and found a remarkable influence of the average molecular weights of the PEP upon the cloud-point pressures. As the polymers studied in this work have weight average molecular weights at least two times higher than the ones analyzed by Chen and Radosz,[15] it seems that phase separation is not appreciably affected by the polymer molecular weight after a certain critical value is reached. This effect may have also been influenced by the high polydispersity of the PP samples analyzed here. As small fractions of polymer chains with very low and very large molecular weights are present in both cases, the LL cloud-point curves may have been determined by the behavior of such small polymer fractions, independently from the weight average molecular weight of the whole polymer samples. From a practical point of view, however, polymers are almost always obtained as a complex mixture of polymer chains of different sizes. For this reason, no attempt was made to prepare polymer samples of low PD.

Figure 6 depicts the Px diagrams for the three PP samples studied here, with 1-butene as solvent at the constant temperature of 150°C. The cloud-point pressures obtained for PP-K (the highest M_w and high PD) are higher and less sensitive to variations of the polymer compositions than the cloud point pressures obtained for the other samples. This is probably due to the higher fractions of chains of large molecular weight in sample PP-K. Sample PP-M (the lowest Mw and PD) led to the lowest cloud point pressure measurements and highest sensitivity to variations of the polymer composition, which is in agreement with the explanation presented before for results obtained with sample PP-K. Although it seems that the sample does influence the results obtained, the effect of the polymer type upon the LL phase separation pressure should not be overemphasized, as differences observed may be regarded as unimportant for most practical reasons. This is particularly true for polymer compositions below the 5 wt % level.

Figure 7 presents cloud-point pressures obtained for PP-T and PP-M, using propylene as the solvent. Comparing Figures 6 and 7 it becomes

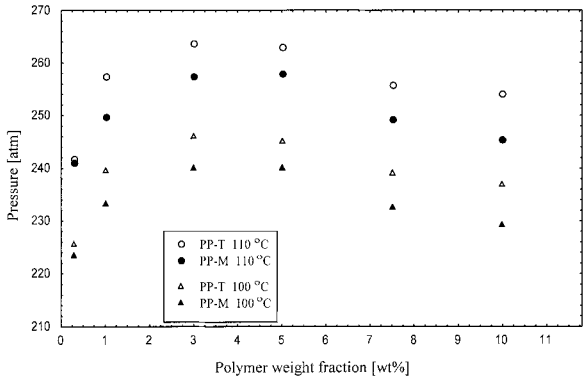

Figure 7 Px diagram (L to LL) for PP-T and PP-M using propylene as the solvent.

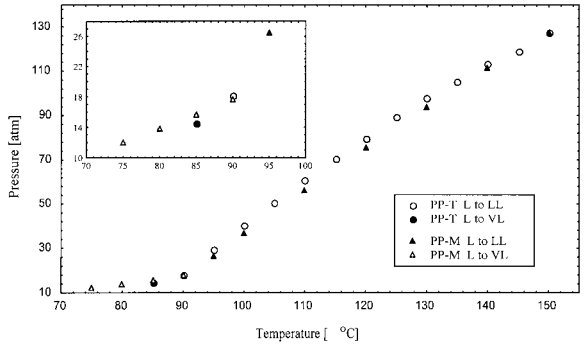

Figure 8 PT diagram for PP-M and PP-T (1 wt %) using 1-butene as the solvent.

clear that the influence of the polymer type upon the L to LL transitions is much more pronounced for C3 than for C4 solvents. This fact may probably be explained in terms of the smaller chain length difference observed for the pair polymer/C4 solvent when compared to the pair polymer/C3 solvent. Once more, though, cloud-point pressures for both samples may be regarded as similar for most practical reasons, as differences observed are always smaller than a few atm.

Figure 8 shows the PT diagram for PP-T and PP-M with 1-butene as the solvent. Two types of transition are presented in Figure 8: liquid to liquid–liquid, and liquid to vapor–liquid. The lower critical end point (intersection of VL and LL curves) curves for both systems are very similar. However, the appearance of the solid phase is about 10°C lower for PP-M than for PP-T. This effect can be explained in terms of the polydispersity of the PP samples. It is known that the increase of the PD causes the increase of the polymer cristallinity and of the melting temperature.[31] In fact, inspection of the DSC diagrams reveals that PP-T has a higher melting temperature than PP-M, which is probably due to the higher PD of PP-T. It may be said that the crystalline phase is more stable for samples of higher PD, which causes the solid liquid transition to occur at higher temperatures for PP-T than for PP-M. In this case, the 10°C difference should not be neglected, as this difference may be very significant for development of actual applications at plant site.

Modeling

In the last decade, the SAFT-EOS has been successfully employed to calculated the phase behavior of systems containing polymers.[14,16–18,32–34] The practical success of the SAFT-EOS is probably due to the more flexible definition of a SAFT fluid. The SAFT fluid is a collection of spherical segments that are exposed to repulsive (hard sphere) and attractive (dispersion) force fields as usual, but that are also able to aggregate through covalent bonds to forms chains (chain effect) and through hydrogen bonds to form short-live clusters (association effect). The main expressions of the SAFT-EOS are presented below, while a detailed description of this equation can be found elsewhere.[27,28]

The SAFT model can be written in terms of the residual Helmholtz energy

$$a^{\text{res}} = a^{\text{ref}} + a^{\text{pert}} \tag{1}$$

where a^{ref} is the reference term and a^{pert} is the perturbation term. The reference part of the SAFT-EOS includes the hard sphere, chain, and association contributions, while the perturbation part accounts for the relatively weaker mean-field dispersion-like effects. The SAFT reference is given by

$$a^{\text{ref}} = a^{\text{hs}} + a^{\text{chain}} + a^{\text{assoc}} \tag{2}$$

As the systems examined here do not exhibit specific interactions that can lead to association, a^{assoc} is set to zero in eq. (2). Huang and Hadosz[27,28] describe the remaining terms presented in eqs. (1)–(2) in detail, for both pure components and mixtures. The interested reader is encouraged to consult the original reference for additional details.

The SAFT-EOS models real molecules as effective chains and characterize them with three parameters: segment number (m, number of segments in each molecule), segment volume (temperature-independent, v^{oo} in mL/gmol of segments), and segment energy (u^o/k in K). Huang and Radosz[27] present pure parameters for a series of substances, as well as general correlations to allow the evaluation of these parameters in the absence of experimental data. The solvent parameters used in this work were taken from this reference. The polymer segment volume was made equal to 12.0 mL/gmol (a value commonly used for polymers). The number of segments was estimated with a generalized correlation for n-alkanes as a function of molecular weight.[27] Afterwards, this parameter was corrected to account for differences between the repeating struc-

Table IV SAFT-EOS Pure Component Parameter

Compound	Molecular Weight	m	v^{00}	u^0/k
Propane	44,097	2.696	13.457	193.03
Propylene	42,081	2.223	15.648	213.90
n-Butane	58,124	3.458	12.599	195.11
1-Butene	56,108	3.162	13.154	202.49
PP-T	245,000	7607	12.000	195.89
PP-K	475,000	14772	12.000	195.89
PP-M	200,000	6065	12.000	195.89

tures of PP and of PE. For instance, the repeating structure of PP has molecular mass around 42 g/gmol, while the repeating structure of PE has a molecular mass about 28 g/gmol. Hence, the estimated m_{PE} (the SAFT segments) was multiplied by 2/3 to obtain the corresponding m_{PP} value. With these two parameters fixed, the energy segment was estimated based on the PVT data obtained by the Tait equation (DIPPR[35]). The parameters used in this work are listed in Table IV.

Phase diagrams were constructed with the SAFT-EOS by performing bubble-point calculations, setting the desired temperature and phase composition. Figure 9(a) presents the Px diagrams for PP-T/1-butene and PP-T/*n*-butane systems, calculated at 150°C with all binary interaction parameters made equal to zero. Although the SAFT-EOS overestimates the cloud-point pressures for the system PP-T/*n*-butane, the model provides the proper qualitative description of the experimental data. The SAFT predictions (no binary information are required by the model) for the system PP-T/1-butene are in excellent agreement with the experimental data. The poor quantitative agreement obtained for PP-T/*n*-butane shows, however, that the SAFT model is not capable of accounting for the solvent effect correctly. The SAFT-EOS pressure predictions for the PP-T/*n*-butane system are slightly higher than pressure predictions for the PP-T/1-butene system. This can be observed more clearly in Figure 9(b), where Px diagrams are presented for the PP-T/propylene and the PP-T/propane systems at 110°C. It can be noticed that model predictions are very good for the PP-T/propane system and poor for the PP-T/propylene system.

Figure 10 shows the SAFT-EOS predictions in the P-T diagram for PP-T/hydrocarbon solvents with polymer concentration kept constant at 5 wt %. The effects discussed before and shown in Figure 9 can be seen very clearly in Figure 10. Nevertheless, although the SAFT-EOS is not able to predict the phase behavior of all systems studied when the binary interaction parameters are set to zero, Figure 10 shows that the slope of the LCST is correctly predicted for all binary PP-T/solvent systems.

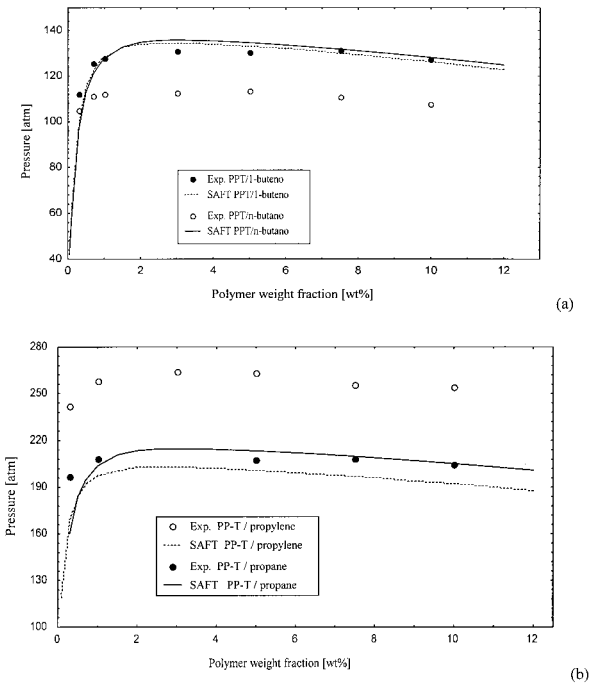

Figure 9 Comparison of experimental and predicted values (SAFT-EOS, $k_{ij} = 0$) in the Px diagram (L to LL, temperature of 150°C) for the (a) PP-T/*n*-butane, PP-T/1-butene, (b) PP-T/propane and PP-T/propylene systems.

Figure 11 presents the P-x diagrams for different PP samples in 1-butene. It can be observed that the SAFT-EOS is able to account for the

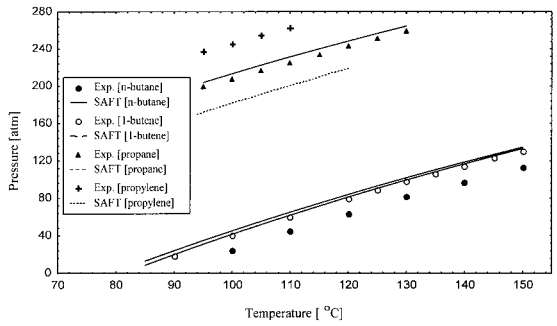

Figure 10 Experimental and SAFT ($k_{ij} = 0$) P-T diagram for PP-T (5 wt %) with hydrocarbon solvents.

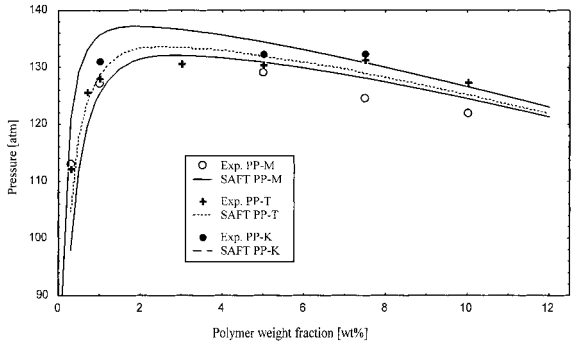

Figure 11 Experimental and SAFT ($k_{ij} = 0$) P-x diagram (temperature of 150°C) with 1-butene as solvent.

effect of the different molecular properties of the polypropylene samples. Both experimental and simulation data indicate that, within the experimental range studied, doubling the polymer molecular weight (from 245,000 for PP-T to 475,000 for PP-K) shifts the cloud-point curve only slightly towards higher pressures.

To improve the description of phase equilibrium, binary interaction parameters, k_{ij}, were estimated with the help of a standard maximum likelihood procedure.[36] (Interaction parameters are used to describe the cross interaction energy between different segments[27,28].) According to the maximum likelihood technique, differences between model predictions and experimental data are weighed with the inverse of the experimental variances, which were obtained through replication of experimental measurements. All experimental data available, covering the whole ranges of polymer composition and temperature, were used to estimate the optimum k_{ij} values. Results obtained for PP-T/hydrocarbon solvents are listed in Table V. For the remaining polymer samples, the binary parameters obtained were very similar to the ones presented in Table V. Therefore, parameters presented in Table V are adequate to describe all experimental data presented here.

Table V Binary Interaction Parameters for PP-T/Hydrocarbon System

Solvent	k_{12} Value
n-Butane	−0.0285
1-Butene	−0.0009
Propane	−0.0005
Propylene	0.0295

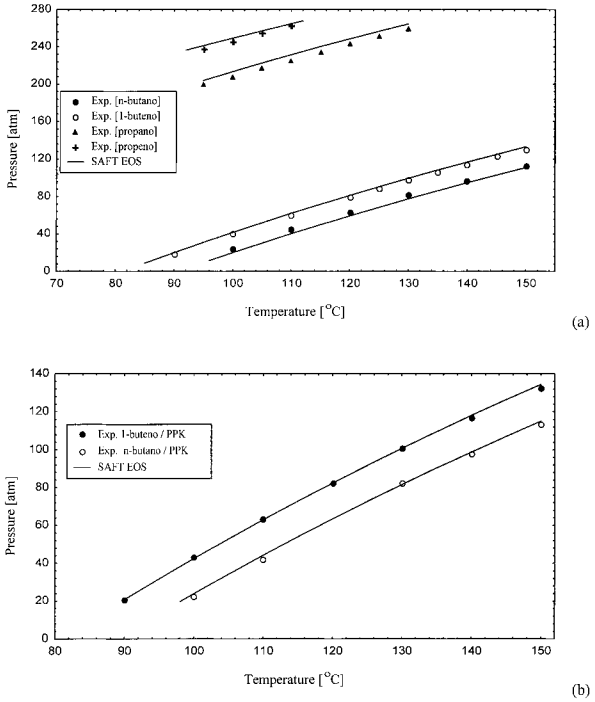

Figure 12 Experimental and calculated P-T diagrams for (a) PP-T and (b) PP-K (5 wt %) with hydrocarbon solvents (k_{ij} values listed in Table V).

Figure 12(a) depicts the PT diagram for PP-T/hydrocarbon solvents at 5 wt % polymer concentration. It is worth noticing that the use of the k_{ij} parameters leads to a remarkable improvement of phase equilibrium representation, allowing the description of the LCST curves for all systems through the SAFT-EOS with an excellent agreement with the experimental data. The k_{ij} parameters estimated from the PP-T systems were used

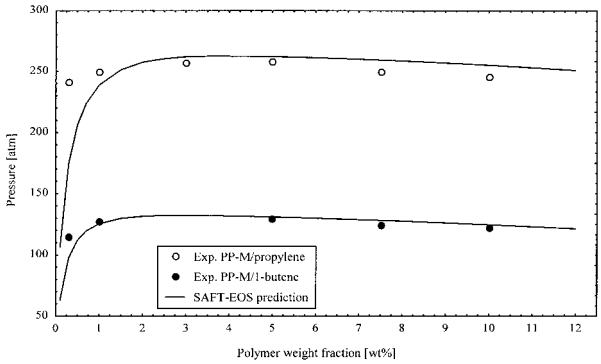

Figure 13 Experimental and calculated P-x diagrams for PP-M/1-butene (T = 150°C) and PP-M/propylene (T = 110°C) systems (k_{ij} values listed in Table V).

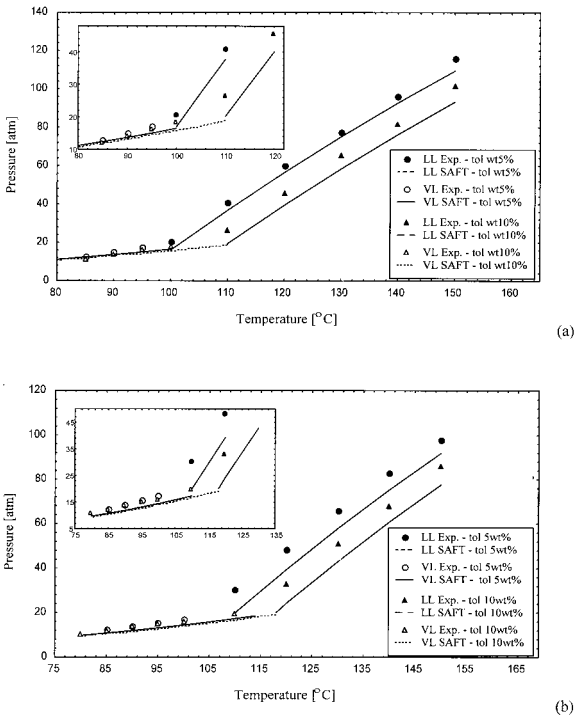

Figure 14 Experimental and calculated P-T diagrams for the ternary systems (a) PP-T (10 wt %)/ toluene/1-butene and (b) PP-T (10 wt %)/toluene/*n*-butane. Apart from the PP-T/1-butene k_{ij} and PP-T/*n*-butane k_{ij}, the other binary interaction parameters were made equal to zero.

to predict the phase behavior of PP-K systems. Figure 12(b) presents the PT diagram of PP-K/1-butene and PP-K/*n*-butane systems, where one can observe the excellent agreement between the SAFT-EOS predictions and the available experimental data. This probably indicates that the binary parameters are not sensitive to changes of the polymer molecular weight. The same good SAFT-EOS predictions can be visualized in Figure 13 for PP-M/1-butene and PP-M/propylene systems.

Figure 14 shows the PT diagrams for the ternary systems PP/toluene/light solvent. Experimental data were presented by Dariva et al.[20] It is important to emphasize that just one binary parameter was used to build the ternary diagrams, as shown in Table V. The remaining binary parameters were made equal to zero. Despite that, the performance of the SAFT-EOS can be considered quite satisfactory, and no additional adjustable parameter is needed to describe these systems. It must be noticed that the SAFT-EOS predicts the LCEP loci with very good accuracy.

CONCLUSIONS

High-pressure phase equilibrium data for different polypropylene samples in propane, propylene, *n*-butane, and 1-butene are provided. Phase transitions were observed visually as cloud points, and are reported for L to VL and L to LL, allowing the construction of the LCST curves for all systems. It was shown that paraffins lead to the decrease of the pressure transition values for all polymer samples analyzed, when pressure transition data obtained for olefins and paraffins of similar chain length and at similar temperatures and polymer compositions are compared. Therefore, the one-phase region is larger for paraffins than for olefins, regardless of the polymer sample analyzed. In the range of commercial interest, it is also observed that the influence of polymer average molecular weight upon the cloud points is negligible. Finally, it is shown that, provided that a global binary parameter for polymer–solvent interaction is estimated, the SAFT-EOS provides excellent fits for available experimental data and may be used successfully for description of the solution behavior in the whole experimental range analyzed.

The authors thank CNPq (Conselho Nacional de Desenvolvimento Científico e Tecnológico) and FAPERJ (Fundação de Apoio à Pesquisa do Estado do Rio de Janeiro) for financial support and for providing scholarships. The authors also thank Polibrasil Resinas S.A. for generously providing the commercial polypropylene samples, and Dr. Humberto Lovisi for preparing the metallocenic polypropylene sample.

REFERENCES

1. Souza, M. E.; Lima, E. L.; Pinto, J. C. Polym Eng Sci 1996, 36, 433.
2. Cavalcanti, M. J. R.; Pinto, J. C. J Appl Polym Sci 1997, 65, 1683.
3. Sayer, C.; Lima, E. L.; Pinto, J. C.; Arzamendi, G.; Asua, J. M. J Polym Sci A Polym Chem 2000, 38, 1100.
4. Canelas, D. A.; Betts, D. E.; DeSimone, J. M. Macromolecules 1996, 29, 2818.
5. Lepilleur, C.; Beckman, E. J. Macromolecules 1997, 30, 745.
6. Hsiao, Y. L.; Maury, E. E.; DeSimone, J. M.; Mawson, S.; Johnston, K .P. Macromolecules 1995, 28, 8159.
7. Srinivasan, G.; Elliot, J. R. Ind Eng Chem Res 1992, 31, 1414.

8. Kontogeorgis, G. M.; Saraiva, A.; Fredenslund, A.; Tassios, D. Ind Eng Chem Res 1995, 34, 1823.
9. Mawson, S.; Johnston, K. P.; Combes, J. R.; DeSimone, J. M. Macromolecules 1995, 28, 3182.
10. Folie, B.; Radosz, M. Ind Eng Chem Res 1995, 34, 1501.
11. Seckner, A. J.; McClellan, A. K., McHugh, M. A. AIChE J 1988, 34, 9.
12. Moore, E. P., Jr.; Larson, G. A. In Polypropylene Handbook; Moore, E. P., Jr., Ed.; Hanser Publishers: Cincinatti, OH, 1996.
13. Kristi, L. A.; Stein, F. P.; Han, S. J.; Gregg, C. J.; Radosz, M. Fluid Phase Equilibria 1996, 117, 84.
14. Xiong, Y.; Kiran, E. J Appl Polym Sci 1995, 55, 1805.
15. Chen, S. J.; Radosz, M. I. Macromolecules 1992, 25, 3089.
16. Chen, S. J.; Economou, I. G.; Radosz, M. Macromolecules 1992, 25, 4987.
17. Gregg, C. J.; Stein, F. P.; Radosz, M. Macromolecules 1994, 27, 4972.
18. Gregg, C. J.; Stein, F. P.; Radosz, M. Macromolecules 1994, 27, 4981.
19. Whaley, P. D.; Winter, H. H.; Ehrlich, P. Macromolecules 1997, 30, 4882.
20. Dariva, C.; Pinto, J. C.; Oliveira J. V. Ind Eng Chem Res 2000, 39, 4627.
21. Zeman, L.; Patterson, D. J Phys Chem 1972, 76, 1214.
22. Zeman, L.; Biros, J.; Delmas, G. Patterson, D. J Phys Chem 1972, 76, 1206.
23. Patterson, D. Rubber Chem Technol 1967, 40, 1.
24. Sanchez, I. C.; Lacombe, R. H. Macromolecules 1978, 11, 1145.
25. Mattedi, S.; Castier, M.; Tavares, F. W. Braz J Chem Eng 1998, 15, 313.
26. Chapman, W. G.; Gubbins, K. E.; Jackson, G.; Radosz, M. Ind Eng Chem Res 1990, 29, 1709.
27. Huang, S. H.; Radosz, M. Ind Eng Chem Res 1990, 29, 2284.
28. Huang, S. H.; Radosz, M. Ind Eng Chem Res 1991, 30, 1994.
29. Dariva, C.; Stuart, G. R.; Oliveira, J. V. Braz J Chem Eng, accepted.
30. Dariva, C. DSc. Thesis, PEQ/COPPE/UFRJ, Rio de Janeiro, 2000 (in Portuguese).
31. Cecchin, G. Macromol Symp 1994, 78, 213.
32. Chen, C. K.; Duran, M. A.; Radosz, M. Ind Eng Chem Res 1994, 33, 306.
33. Folie, B. AIChE J 1996, 42, 3466.
34. Wu, C. S.; Chen, Y. P. Fluid Phase Equilibria 1994, 100, 103.
35. Danner, R. P.; High, M. S. Handbook of Polymer Solution Thermodynamics, AIChE, 1993.
36. Noronha, F. B.; Pinto, J. C.; Monteiro, J. L.; Lobãto, M. W.; Santos, T. J. Um Pacote Computacional perca Estimação de Parâmetros e Projeto de Experimentos, Technical Report COPPE/UFRJ, Rio de Janeiro, 1993.